Radiology

Lung Abnormalities Depicted with Hyperpolarized Xenon MRI in Patients with Long COVID

Manuscript Type: Original Research

Authors: James T. Grist BSc PhD1,2,3,4, Guilhem J. Collier PhD5, Huw Walters MBBS 1, Minsuok Kim PhD6, Mitchell Chen BMBCh MEng DPhil FRCR1, Gabriele Abu Eid BSc1, Aviana Laws1, Violet Matthews BSc1, Kenneth Jacob BSc1, Susan Cross BSc1, Alexandra Eves BSc1, Marianne Durant BSc1, Anthony Mcintyre BAppSci1, Roger Thompson PhD7, Rolf F. Schulte PhD8, Betty Raman MBBS DPhil3, Peter A. Robbins PhD2, Jim M. Wild PhD MSc MA5, Emily Fraser PhD MBChB BSc9, Fergus Gleeson MBBS1,10.

Affiliations:

1 Department of Radiology, Oxford University Hospitals NHS Trust, Oxford, UK

2 Department of Physiology, Anatomy, and Genetics, University of Oxford, UK

3 Radcliffe Department of Medicine, Oxford Centre for Clinical Magnetic Resonance Research, University of Oxford, UK

4 Institute of Cancer and Genomic Sciences, University of Birmingham, Birmingham, UK

5 POLARIS, Department of Infection Immunity and Cardiovascular Disease, University of Sheffield

6 Wolfson School of Mechanical, Electrical and Manufacturing Engineering, Loughborough University

7 Department of Infection, Immunity, and Cardiovascular Disease, University of Sheffield

8 GE Healthcare, Munich, Germany

9 Oxford Interstitial Lung Disease Service, Oxford University Hospitals NHS Trust, Oxford, UK

10 Department of Oncology, University of Oxford, Oxford

Corresponding Author:

Professor Fergus Gleeson, Department of Oncology, University of Oxford.

fergus.gleeson@oncology.ox.ac.uk

Summary

Hyperpolarized xenon 129 MRI and total lung diffusion capacity for carbon monoxide demonstrate significantly impaired gas transfer in non-hospitalized post-COVID-19 condition participants with normal chest CT examinations.

Key Results

1. In a prospective study with 11 participants, there were significant differences in mean red blood cell: tissue plasma between healthy controls and post-hospitalized COVID/non-hospitalized long COVID participants indicating potential differences in lung function.
2. Non-hospitalized long COVID participants had near-normal CT scores, and DLco (%) was significantly lower between NHLC and PHC participants, potentially indicating a decrease in lung function but not structure.

Abbreviations:

Full-scale airway network modelling analysis – FAN

Hyperpolarized ^{129}Xenon MRI - Hp-XeMRI

Non-hospitalised Post-Covid-19 condition - NHLC

Post-hospitalised COVID-19 – PHC

DLco% - Total lung diffusion capacity for carbon monoxide percent predicted for age and sex

RBC:TP - Hyperpolarized ^{129}Xenon MRI lung ratio of red blood cell spectral peak to tissue phase spectral peak

modified Borg score- mBORG

FEV1%- Forced Expiratory Volume in one second percent predicted for age and sex

See also the editorial by Parraga and Matheson.

Abstract

Background

Post-Covid-19 condition describes symptoms following COVID-19 infection after four weeks. Symptoms are wide-ranging but breathlessness is common.

Purpose

The purpose of this study was to determine whether the previously described lung abnormalities on Hp-XeMRI in post-hospitalised COVID-19 participants are also present in non-hospitalised participants with Post-Covid-19 condition.

Methods

In this prospective study, non-hospitalised Post-Covid-19 condition (NHLC) and post-hospitalised COVID-19 (PHC) participants were enrolled from 06/2020 to 08/2021. Participants had chest CT, hyperpolarized pulmonary ^{129}Xenon MRI (Hp-XeMRI), pulmonary function tests, 1-minute sit-to-stand test and breathlessness questionnaires. Control subjects underwent HP-XeMRI only. CT scans were analysed for post COVID interstitial lung disease severity using a previously published scoring system, and Full-scale Airway Network (FAN) modelling. Analysis used group and pair-wise comparisons between participants and controls, and correlations between participant clinical and imaging data.

Results

A total of 11 NHLC (4:7 Male: Female, 44 ± 11 years, [37-50], (mean ± SD, [95% CI]) and 12 PHC (10:2, Male: Female, 58 ± 10 years, [52-64]) participants were included, with a significant difference in age between groups, p = 0.05. NHLC participants were 287 ± 79, [240-334] and PHC 143 ± 72, [105-190] days from infection, respectively. NHLC and PHC participants had normal or near normal CT scans (0.3/25 ± 0.6, [0-0.63] and 7/25 ± 5, [4-10], respectively). Gas transfer (DLco (%)) was different between NHLC and PHC participants (76 ± 8%, [73-83] vs 86 ± 8%, [80-91] respectively, p = 0.04) but there was no evidence of other differences in lung function. Red Blood Cell:Tissue Plasma (RBC:TP) mean was different between volunteers vs PHC (0.45 ± 0.07, [0.43-0.47] vs (0.31 ± 0.10, [0.24-0.37], respectively, p = 0.02) and volunteers vs NHLC (0.37 ± 0.10, [0.31-0.44], p = 0.03) participants, but

not between NHLC and PHC participants (p = 0.26). FAN results did not correlate with DLco or Hp-XeMRI.

Conclusion

NHLC and PHC subjects showed Hp-XeMRI RBC:TP abnormalities, with NHLC participants demonstrating lower DLco than PHC participants despite having normal CT scans.

Introduction

On 11th March 2020, COVID-19 was declared a global pandemic by the World Health Organisation (WHO). Beyond the acute respiratory manifestations of COVID-19 infection, which can result in severe illness, hospitalisation and death, the medium and long-term problems experienced by people following COVID-19 can be considerable(1). Large cohort studies have revealed that symptoms can persist months after initial infection in both participants hospitalised with COVID-19 pneumonia and those managed in the community. The presence of ongoing symptoms related to prior COVID-19 infection has been defined by the World Health Organization as the Post-Covid-19 condition. Although over 200 symptoms have been reported, the most common problems are that of breathlessness, fatigue and brain fog(2). Post-Covid-19 condition presents a global health burden, with many people unable to return to normal activities or employment months after becoming unwell.

The Chest X-ray (CXR) is the most commonly used imaging modality for the diagnostic work-up of acute COVID-19 pneumonia and is often repeated three months after the acute infection in those patients requiring hospital admission. Chest CT may be performed to investigate persistent breathlessness if the CXR is normal, or there are other concerns regarding COVID-19-related lung damage. In a small proportion of participants, interstitial lung abnormalities persist and evidence of post-COVID fibrosis has been reported (3,4). These abnormalities may account for dyspnea, but in the majority of individuals with Post-Covid-19 condition, CT scans are normal or near normal. Similarly, lung function tests are usually within the normal range. A recent study looking at a small cohort of post-hospitalised COVID-19 participants at 3 months, reported that hyperpolarised Xenon ^{129}MRI (Hp-XeMRI), was able to detect abnormalities of alveolar gas transfer even when the CT scans and lung function tests were normal or near normal(5). HP-XeMRI enables the assessment of ventilation and gas transfer across the alveolar epithelium into red blood cells. It provides regional information of pulmonary vasculature integrity and may be able to identify lung abnormalities not apparent on CT(6).

In the Post-Covid-19 condition, a breathing pattern disorder is commonly identified and contributes to breathlessness in a significant proportion of patients(7), however, whether or not there are additional reasons for their breathlessness remains unclear. The purpose of this study was to determine

whether the previously described lung abnormalities on Hp-XeMRI in post-hospitalised COVID-19 participants are also present in non-hospitalised participants with Post-Covid-19 condition(5).

Methods

Patient recruitment and screening

This prospective study was approved by the Healthy Research Authority (HRA) (Research Ethics Committee reference 20/NW/0235), and all participants gave written informed consent. Consecutive participants were recruited from the Oxford Post-COVID Assessment clinic, with the following inclusion criteria:

A) Post-hospitalised COVID (PHC) participants: rt-PCR proof of SARS-CoV-2 infection; no history of intubation; more than 3 months post discharge; no prior history of interstitial lung or airways disease* or a smoking history >10 pack years; and a normal or near normal CT scan.

B) Non-hospitalised Post-Covid-19 condition (NHLC) participants: rt-PCR or positive antibody proof of SARS-CoV-2 infection; not hospitalised during acute infection; no evidence of interstitial lung or airways disease*, or a smoking history >10 pack years; and a normal or near normal CT scan.

For both cohorts, diagnosis of Post-Covid-19 condition was made after referral to a specialist clinic with medically unexplained dyspnea as a symptom, and in accordance with National Institute for Health and Care Excellence diagnostic criteria.

C) Healthy volunteers were recruited from the local staff pool at the University of Sheffield and the University of Oxford. Volunteers had to have no previous evidence of COVID-19 infection with rt-PCR testing and no significant history of lung or cardiovascular disease or smoking. We did allow for the inclusion of mild well-controlled asthmatic volunteer with no evidence of airways obstruction on spirometry (Figure 1).

Imaging protocol and physiological measurements

Imaging was performed at 1.5T (HDx, GE Healthcare, Chicago, IL) using a dedicated xenon Transmit/Receive coil (CMRS, Brookfield, WI) and ^{1}H images acquired on the body coil. When possible, participants underwent two HP-XeMRI scans, with the second performed approximately one hour later.

A 3D 4-echo flyback radial acquisition was used to acquire dissolved phase hyperpolarized ^{129}Xe Images as previously described(3,6). Sequence parameters were: single breath hold, acquired/reconstructed image resolution of 1.75/ .875 cm in all dimensions, repetition time per spoke = 23ms, nominal flip angle per excitation on dissolved and gas phases = 40 and 0.7 degrees, respectively, total scan time = 16s. Gas, Tissue/Plasma (TP), and Red Blood Cell (RBC) images were reconstructed.

The noise level for each image was calculated on a slice-by-slice basis. Any voxels in the TP mask in each slice that were less than 5 times the median noise level in the slice were discarded. Ratiometric maps (RBC:TP) were then calculated on a voxel-by-voxel basis. The mean, standard deviation, and coefficient of variation of each ratiometric map was then calculated on a participant-by-participant basis.

All trial participants underwent a contemporaneous low dose Computed Tomography (CT) scan (GE Healthcare, Chicago, IL) following inspiration of 1L of room air, with slice thickness of 0.625mm. Images were reviewed by a radiologist (H.W) with 5 years of experience, blinded to clinical data and Xenon results, as previously described(5). A subset of participants' CT data (9 NHLC and 5 PHC) underwent full-scale airway network modelling analysis (FAN) using the technique as previously reported (9).

They also underwent a hemoglobin (Hb, g/L) assessment, spirometry, gas transfer and Dyspnea-12 score and 1 minute sit-to-stand test (STST). The number of repetitions were recorded, alongside the modified Borg (mBORG) score and oxygen saturations pre and post a one-minute sit-to-stand test.

Statistical analysis

Initial analysis was performed on each participant cohort independently with correlation between clinical and imaging variables assessed using Spearman's correlation, with a subsequent linear fit performed for significantly correlated variables. Correlations between DLco, mean RBC:TP and FAN analysis parameters were performed using Spearman's correlation. The Mann-Whitney U test was used to assess for differences in FAN parameters between NHLC and PHC cohorts.

Participant data was separated into non-hospitalised Post-Covid-19 condition (NHLC) and post-hospitalized COVID (PHC) groups and the above analysis re-performed for group-dependent associations with clinical symptoms.

Comparisons between RBC:TP in participants and volunteer groups was assessed using a non-parametric ANOVA and Tukey post hoc tests with Bonferroni correction for multiple comparisons. Where data was only available for participants, for example mBORG and lung function data, a two-sided t-test was used to compare between cohorts. The Intra Class Correlation Coefficient (ICC) was calculated to assess repeatability of mean RBC:TP using data from the repeated HP-XeMRI scans. A p value of $< .05$ was assumed for statistical significance. All analysis was performed in R (The R Project, The R Foundation, Vienna, Austria). Unless otherwise stated, all data are presented as mean ± SD [95% CI].

Results

Participant characteristics

A total of 11 NHLC (7 female) and 12 PHC (2 female) participants were recruited, with a mean age of 44 ± 1, [37-50] years and 58 ± 10, [52-64] years ($p = 0.05$), respectively. CT, proton, and fused RBC:TP and proton images from participants with NHLC and PHC are shown in Figures 2 and 3, respectively. Thirteen healthy volunteers (mean age: 41 ± 11, [30-52] years, 6 female) were recruited and underwent Hp-XeMRI. Example proton and fused RBC:TP and proton images for a volunteer in this study are shown in Supplementary Figure 1. The mean time from infection for the NHLC and PHC participants was 287 ± 79 [240-334] and 149 ± 68 [105-190] days ($p < 0.01$), respectively.

Average Hb for NHLC and HLC was 144 ± 15, [134-153] g/L and 145 ± 14, [133-150] g/L, respectively. NHLC and PHC participants exhibited breathlessness with a mean Dyspnea-12 score of 9 ± 5 [6-12] and 10 ± 5 [7-12] ($p = 0.67$) and mBORG pre- and post-sit stand test of 2 ± 2 [0.8-3] and 7 ± 1 [6-7] and 2 ± 2 [0.5-3] and 5 ± 1 [4-6], respectively ($p > 0.05$ in all cases). There was no evidence of differences in oxygen saturations before and after mBORG sit-stand test (97.06 ± 0.02%, [96-98] vs 97.59 ± 0.02%, [97-99] oxygen saturation before vs after, $p = 0.99$). The majority (9/11 and 4/5) of NHLC and PHC participants were in the bottom 2.5th percentile for the number of repetitions they could do for the mBORG sit-stand test, range 2.5-75 and range 2.5-25, respectively(10). There were

significant differences between NHLC and the PHC participants' CT score (0.3 ± 0.6 [0-0.6] and 7 ± 5 [4-11] respectively, $p < 0.01$).

Lung function and Imaging results

The mean, standard deviation, and coefficient of variation of NHLC, PHC participants, and healthy volunteers RBC:TP are shown in Figure 4. There were significant differences in RBC:TP mean between volunteers (0.46 ± 0.07, [0.43-0.47]) and PHC (0.31 ± 0.10, [0.24-0.37]) and volunteers and NHLC (0.37 ± 0.10, [0.31-0.44]) participants (adjusted $p<0.05$ in all cases), however not between PHC and NHLC ($p = 0.29$). Of note, 7/11 of NHLC and 11/12 of PHC participants were beyond 2 standard deviations of the mean from normal volunteer mean RBC:TP.

There was no significant difference in mean percent Forced Expiratory Volume (FEV) between100 ± 13%, [92-108] and 88 ± 21%, [72-97] ($p>0.05$), or FVC but there was a significant difference mean gas transfer (DLco), 78 ± 8%, [73-84] vs 86 ± 9%, [80-91] ($p = 0.04$) between NHLC and PHC participants respectively.

In NHLC participants, there was a significant correlation between DLco (%) and RBC:TP standard deviation (cc = 0.78, $p = 0.02$), RBC:TP mean and RBC:TP standard deviation (cc = 0.63, $p = 0.05$). Further correlations between RBC:TP and Dyspnea-12 score and RBC:TP and mBORG post-sit stand were close to significance ($p = 0.06$ and 0.08, respectively). Correlations between RBC:TP mean and RBC:TP standard deviation in Supplementary Figure 2A, and DLco (%) and RBC:TP standard deviation in Figure 5A.

There were significant correlations in the PHC participants between participant age and the dissolved phase mean (cc = -0.82, $p < 0.01$, Supplementary Figure 2B), CT score and RBC:TP standard deviation (cc = 0.54, $p = 0.04$, Figure 5B), RBC:TP mean and RBC:TP standard deviation (cc = 0.76, $p = 0.03$, Supplementary Figure 2C), and RBC:TP mean and RBC:TP coefficient of variation (cc = -0.73, $p = 0.04$, Supplementary Figure 2D). 10 PHC participants underwent repeat HP-Xe imaging and the ICC of mean RBC:TP was 0.96 [0.87-0.99] [lower-upper bound], indicating excellent repeatability, see Supplementary Table 1(11). There were no significant correlations between DLco (%), mean RBC:TP and any of the FAN parameters. There was also no evidence of differences between FAN

parameters in the 9 NHLC and 5 PHC participants (all p>0.1). FAN modelling results are shown in Figure 6.

Discussion

This pilot study utilised Hp-XeMRI to evaluate the lungs of NHLC participants with unexplained breathlessness following clinical evaluation in a dedicated post-COVID clinic. We found that the NHLC participants had normal CT scans, and the PHC had normal or near normal CT scans (0.3/25 ± 0.6 [0-0.6] and 7/25 ± 5 [4-11], respectively). Gas transfer (DLco (%)) was significantly different between NHLC and PHC participants (76 ± 8%, [73-84] vs 86 ± 8%, [80-91], respectively, p = .04) but there was no evidence of other differences in lung function. Red Blood Cell:Tissue Plasma (RBC:TP) mean was significantly different between volunteers (0.45 ± 0.07, [0.43-0.47]) vs PHC (0.31 ± 0.10, [0.24-0.37], p = 0.02) and volunteers vs NHLC (0.37 ± 0.10, [0.31-0.44], p = 0.03) participants, but not between NHLC and PHC participants (p = 0.26).

All the NHLC participants in this study with abnormal Hp-XeMRI were imaged more than 6 months after their initial infection, indicating that these abnormalities were not a transient phenomenon following acute infection. The NHLC participants were also on average further from their initial infection than the PHC group (287 v 149 days). Interestingly, the measured abnormality on Hp-XeMRI appears to be only marginally greater in the PHC than the NHLC participants despite those admitted to hospital having had a presumed clinically more severe acute infection.

The participants in this study were well phenotyped with symptoms typical of non-hospitalised Post-Covid-19 condition participants who did not require hospital admission(12). The relationship of the Hp-XeMRI abnormalities detected and the breathlessness experienced by the wider population of Post-Covid-19 condition participants, managed both in hospital and in the community during their acute infection is unclear. Additionally, the pathophysiological mechanisms that underlie the changes in Hp-XeMRI post COVID-19 infection remain to be fully elucidated. Although, it is possible to make some inferences regarding the nature of the underlying defect based on our results. It is known that inert gases (those that do not chemically react with blood) equilibrate rapidly in the lung(13), with Xenon

quickly reaching the red blood cells(14). RBC:TP is a composite of the ratio of two tissue volumes (the pulmonary capillary (plus potentially some pulmonary venous) blood volume to the alveolar membrane volume), gas transfer, and pulmonary blood flow - measured using Hp-XeMRI. A lower figure suggesting that infection with Sars-CoV-2 may have induced some microstructural abnormality to either one or both volumes, causing a reduction in blood volume for example due to widespread microclots(15), changes in pulmonary blood flow, and/or a thickening of the alveolar membrane, both of which would be expected to cause a reduction in diffusing capacity(16).

It is potentially possible that in participants hospitalised with COVID-19 pneumonia, our PHC group, that the direct damage to the lungs caused by the virus and resultant inflammatory sequelae may cause longer-lasting microstructural abnormalities. Indeed, although the CT scans were normal or near normal in the PHC participants, a faint 'footprint' of prior COVID-19 pneumonia, when present, may possibly at least partially explain the abnormal RBC:TP and pulmonary gas transfer values. In contrast, in the NHLC participants, all the CT scans were normal and none of the participants had evidence of having had pneumonia (accepting that this may have been because they were not imaged during their acute infection). This could potentially indicate that the abnormalities detected in the NHLC cohort have a different pathophysiological basis. Furthermore, the gas transfer (DL_{CO}), which also provides a measure of pulmonary vascular integrity, was lower in the NHLC group than the PHC group and correlates with the RBC:TP ratio, reinforcing the significance of the findings and the need for further investigation to delineate the nature of the abnormality. To further reinforce the reliability of these results, we note that previous findings have shown Xenon MRI to be a reproducible technique in both participants and volunteers, and show a similar decreased RBC:TP as previously seen (3). We also performed repeat imaging in a subset of PHC participants and again confirmed excellent repeatability of mean RBC:TP.

Outside the setting of SARS-CoV2 infection it is known from prior studies with Hp-XeMRI in participants with CT diagnosed interstitial lung disease that more severe disease determined by DL_{CO} correlates with worsening RBC:TP and that Hp-XeMRI may identify lung abnormality in areas that are normal on CT(17). Hp-XeMRI appears to also be a more sensitive way of detecting disease than CT in participants with Post-Covid-19 condition and may be a useful tool in its diagnosis, quantification

and follow-up. But caution is necessary as it is unknown whether participants with other respiratory tract infections such as flu have abnormal Hp-XeMRI gas transfer months after infection even when non-hospitalised and with a normal CT. It is also not known whether the abnormalities we have detected are of clinical significance, nor whether Hp-XeMRI is an over-sensitive test, although the correlation with DL_{CO} argues against this.

The FAN model has been shown to accurately reflect regional ventilation(9). The recent paper using FAN modelling in patients post COVID-19 pneumonia has confirmed that in patients with normal CT scans that there are no significant detectable ventilation changes(18). The lack of significant correlation between FAN and dissolved phase imaging we are reporting is in keeping with this, suggesting that in patients without detectable CT abnormalities, it is the presence of continuing pathology in the microvasculature and walls of the alveolar sac, as the cause of the ongoing breathlessness in Post-COVID-19 dyspnea.

There are limitations to this study. Only a small cohort of PHC and NHLC participants were examined. Extrapolating these results to the worldwide population with breathlessness associated with the Post-Covid-19 condition needs to be performed with caution. We note that a power analysis showed a need for 4 more participants in the NHLC cohort to begin to see statistical associations between RBC:TP and quality of life scores. Furthermore, there is a need to repeat this study in a similar cohort at another site, using power calculations(19). Older NHLC patient should be included in further studies, to better assess for differences in RBC:TP with age. To better understand the significance of our findings, in the future we plan to recruit a larger cohort of participants that includes NHLC participants without significant breathlessness alongside participants with prior proven COVID-19 infection who have fully recovered. We will also be performing repeat imaging at different time intervals up to 12 months to determine whether the abnormalities detected persist or resolve over time.

In conclusion, Hp-XeMRI has identified objective impairment in gas transfer in the lungs of non-hospitalised dyspneic Post-Covid-19 condition participants with normal CT scans, providing preliminary evidence that lung abnormalities exist that cannot be detected with conventional imaging.

The significance and underlying pathophysiology of this abnormality is currently unknown and highlights the need for further research in this field.

Acknowledgements:

This work was funded by the University of Oxford, the Oxford NIHR Biomedical Research Centre, the National Consortium of Intelligent Medical Imaging, the National Institute of Health Research, and the British Heart Foundation Oxford Centre of Research Excellence. We would like to thank the C-MORE research team for their support of this study. The Sheffield collaborators are also supported by MRC/ MR/M008894/1. We would like to thank Barry Johnson for his help and support in this study.

References

1. Huang C, Huang L, Wang Y, et al. 6-month consequences of COVID-19 in patients discharged from hospital: a cohort study. Lancet. Elsevier Ltd; 2021;397(10270):220–232. doi: 10.1016/S0140-6736(20)32656-8.
2. World Health Organization. A clinical case definition of post COVID-19 condition by a Delphi consensus, 6 October 2021. 2021;(October):27. file:///C:/Users/pbradley/Downloads/WHO-2019-nCoV-Post-COVID-19-condition-Clinical-case-definition-2021.1-eng.pdf.
3. Han X, Fan Y, Alwalid O, et al. Six-Month Follow-up Chest CT findings after Severe COVID-19 Pneumonia Manuscript type: Original Research. (1).
4. Pan F, Yang L, Liang B, et al. Chest CT Patterns from Diagnosis to 1 Year of Follow-up in Patients with COVID-19. Radiology. 2022;302(3):709–719. doi: 10.1148/radiol.2021211199.
5. Grist JT, Chen M, Collier GJ, et al. Hyperpolarized 129Xe MRI Abnormalities in Dyspneic Participants 3 Months after COVID-19 Pneumonia: Preliminary Results. Radiology. 2021;0(June):0.
6. Qing K, Ruppert K, Jiang Y, et al. Regional mapping of gas uptake by blood and tissue in the human lung using hyperpolarized xenon-129. J Magn Reson Imaging. 2014;39(2):346–359. doi: 10.1002/jmri.24181.Regional.
7. Motiejunaite J, Balagny P, Arnoult F, et al. Hyperventilation as one of the mechanisms of persistent dyspnoea in SARS-CoV-2 survivors. Eur Respir J. 2021;58(2). doi: 10.1183/13993003.01578-2021.
8. Collier GJ, Eaden JA, Hughes PJC, et al. Dissolved 129Xe lung MRI with four-echo 3D radial spectroscopic imaging: Quantification of regional gas transfer in idiopathic pulmonary fibrosis. Magn Reson Med. 2020;(October):1–12. doi: 10.1002/mrm.28609.
9. Kim M, Doganay O, Matin TN, Povey T, Gleeson F V. CT-based Airway Flow Model to Assess Ventilation in Chronic Obstructive Pulmonary Disease: A pilot study. Radiology. 2019;293(3):666–673. doi: 10.1148/radiol.2019190395.
10. Strassmann A, Steurer-Stey C, Lana KD, et al. Population-based reference values for the 1-min sit-to-stand test. Int J Public Health. 2013;58(6):949–953. doi: 10.1007/s00038-013-0504-z.

11. Koo TK, Li MY. A Guideline of Selecting and Reporting Intraclass Correlation Coefficients for Reliability Research. J Chiropr Med. Elsevier B.V.; 2016;15(2):155–163. doi: 10.1016/j.jcm.2016.02.012.
12. NICE, RCGP and SIGN publish guideline on managing the long-term effects of COVID-19. 2020. https://www.nice.org.uk/news/article/nice-rcgp-and-sign-publish-guideline-on-managing-the-long-term-effects-of-covid-19.
13. Piiper J, Scheid P. Blood-gas equilibration in lungs. In: Pulmonary Gas Exchange. Academic Press Inc; 1980.
14. Stewart NJ, Leung G, Norquay G, et al. Experimental validation of the hyperpolarized (129) Xe chemical shift saturation recovery technique in healthy volunteers and subjects with interstitial lung disease. Magn Reson Med. 2014;00(July). doi: 10.1002/mrm.25400.
15. Pretorius E, Vlok M, Venter C, et al. Persistent clotting protein pathology in Long COVID/Post-Acute Sequelae of COVID-19 (PASC) is accompanied by increased levels of antiplasmin. Cardiovasc Diabetol. BioMed Central; 2021;20(1):1–18. doi: 10.1186/s12933-021-01359-7.
16. Roughton F., Forster RE. Relative importance of diffusion and chemical reaction rates in determining rate of exchange of gases in the human lung, with special reference to true diffusing capacity of pulmonary membrane and volume of blood in the lung capillaries. J Appl Physiol. 1957;11:290–302.
17. Mammarappallil J, Rankine L, Wild JM, Driehuys B. New Developments in Imaging Idiopathic Pulmonary Fibrosis With Hyperpolarized Xenon Magnetic Resonance Imaging. J Thorac Imaging. 2019;34(2):136–150.
18. Inui S, Yoon SH, Doganay O, Gleeson F V., Kim M. Impaired pulmonary ventilation beyond pneumonia in COVID-19: A preliminary observation. PLoS One. 2022;17(1 1):1–13. doi: 10.1371/journal.pone.0263158.
19. Eng J. Sample size estimation: how many individuals should be studied? Radiology. 2003;227:309–313. doi: 10.1148/radiol.2272012051.

Figures

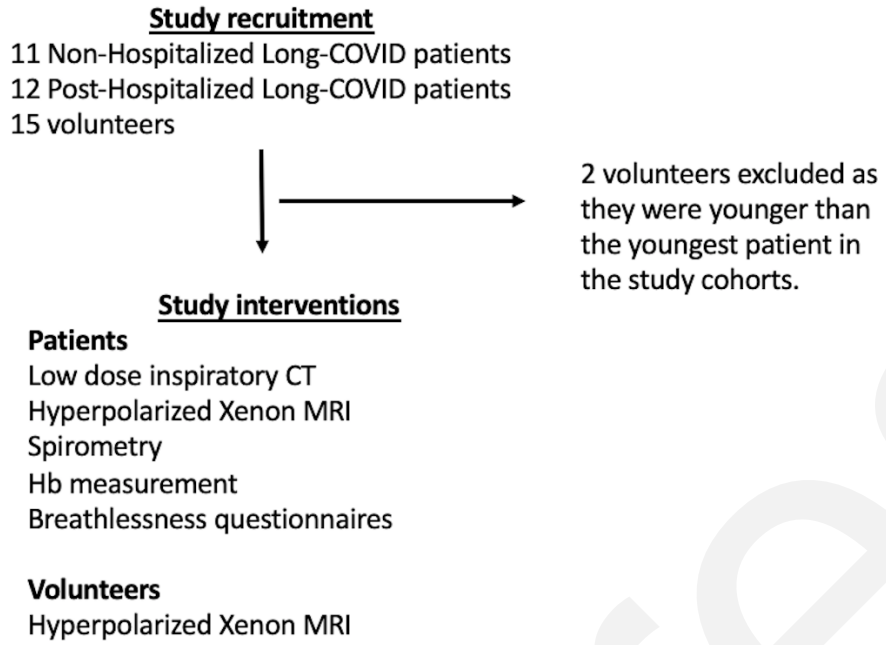

Figure 1. The study flowchart.

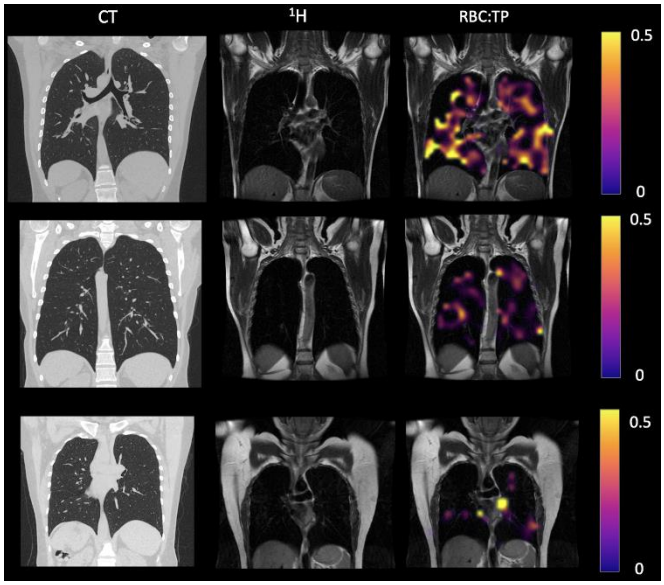

Figure 2. Example CT, proton, proton and RBC:TP imaging from Post-Covid-19 condition participants. The top row is a participant with RBC:TP = 0.49, the middle row is a participant with RBC:TP of 0.31, and the bottom row is a participant with RBC:TP = 0.24. Imaging showed little to no discernible damage on CT, and yet highly heterogeneous and low RBC:TP in the lungs of NHLC participants.

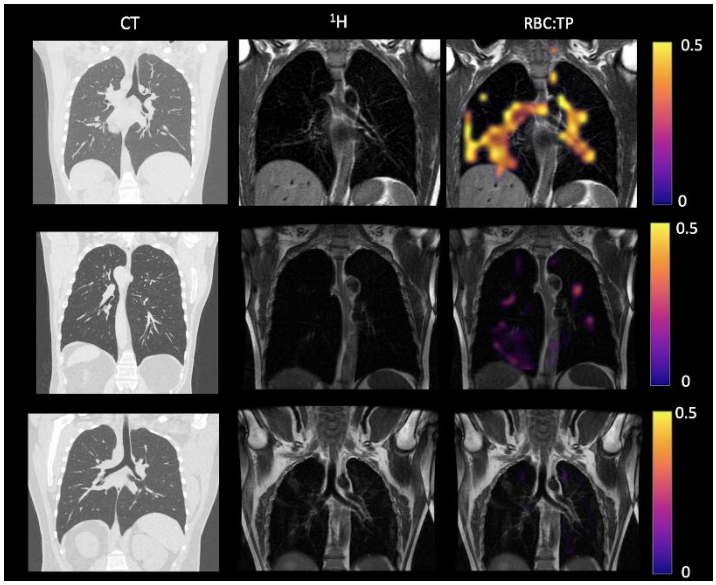

Figure 3. Example CT, proton, proton and RBC:TP imaging from post-Hospitalized participants. The top row is a participant with RBC:TP = 0.59, the middle row is a participant with RBC:TP of 0.31, and the bottom row is a participant with RBC:TP = 0.16. Imaging showed minimal damage on CT, and yet highly heterogeneous and low RBC:TP in the lungs of post-Hospitalized participants.

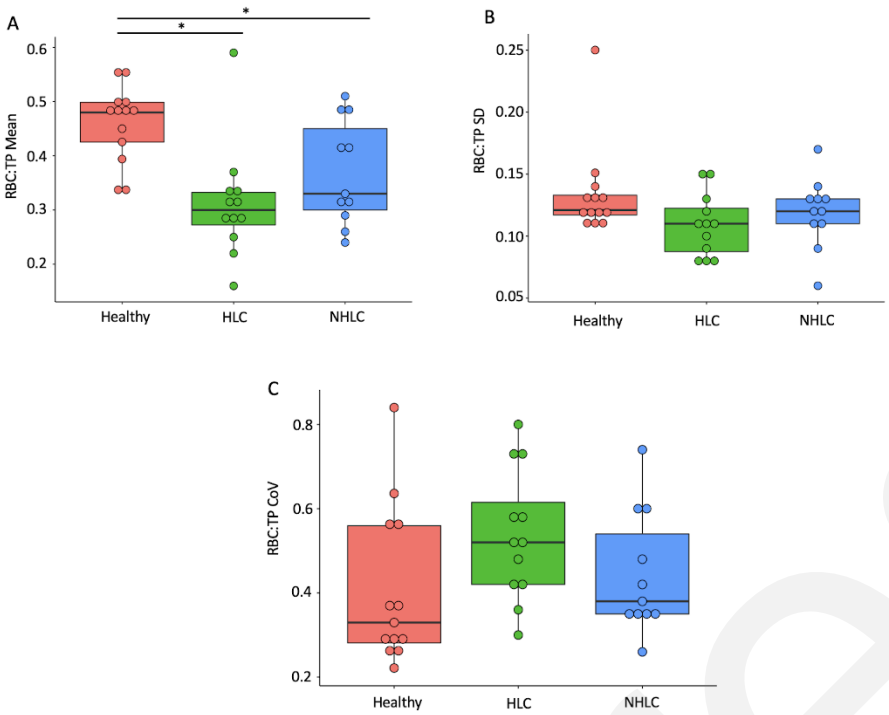

Figure 4. Comparison of RBC:TP mean **(A)**, standard deviation (SD) **(B)**, and Coefficient of Variation **(C)** between healthy, post-hospitalized COVID, and non-hospitalized Post-Covid-19 condition participants. * = significant after correction for multiple comparisons. Results show a significant decrease in RBC:TP in participants in comparison to controls.

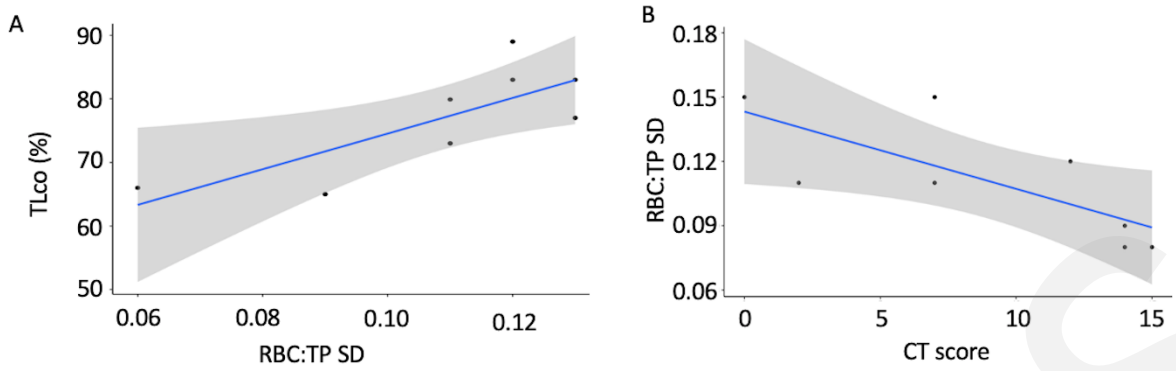

Figure 5. Correlation results. **(A)** A significant positive correlation between DLco (%) and RBC:TP Standard Deviation (STD) in the NHLC group. **(B)** a significant positive correlation between RBC:TP Standard Deviation (SD) and CT score in the PHC group. Results demonstrate that abnormally low gas transfer measurements are linked to changes in RBC:TP.

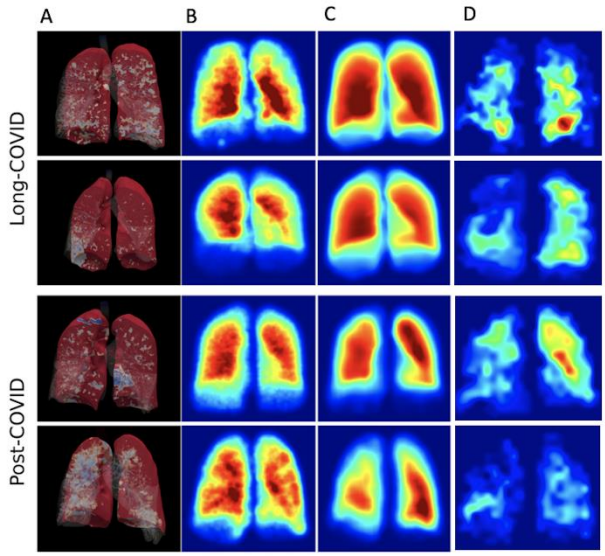

Figure 6. 3D render of FAN **(A)**, FAN modelling **(B)**, and hyperpolarized Xenon imaging **(C, D)** in both NHLC and PHC participants. Results from both the low-resolution and ventilation imaging are similar and did not correlate with clinical or dissolved phase imaging results.

Tables

Table 1. Data for Each Long-COVID Participant

ID	Age at scan (years)	Gender	Hb (g/L)	Time from infection (days)	FEV (%)	TLco(%)	CT Score	RBC:TP Mean	RBC:TP STD	RBC: TP Coeff Var	Dysp -12	mBORG pre	mBORG post	Number of resps in one minute	Percentile for Age and Sex
1	61	M	141	210	104	80	0	0.31	0.31	0.34	N/A	0	7	21	2.5
2	39	M	161	393	106	N/A	0	0.49	0.14	0.28	5	0	5	58	75
3	39	F	125	437	102	77	0	0.32	0.13	0.40	10	1	8	30	2.5
4	51	F	N/A	394	123	N/A	0	0.42	0.13	0.31	11	2	8	30	2.5
5	28	M	166	263	72	83	0	0.51	0.13	0.27	0	0	5	18	2.5
6	46	F	122	213	98	73	0	0.24	0.11	0.47	7	5	8	21	2.5
7	59	F	142	260	105	89	2	0.29	0.12	0.40	16	3	7	27	2.5
8	55	F	145	261	97	65	0	0.33	0.09	0.27	7	3	8	22	2.5
9	34	F	143	294	101	83	1	0.41	0.12	0.28	12	3	7	61	75
10	38	F	128	246	83	66	0	0.26	0.06	0.23	21	3	6	21	2.5
11	29	M	166	166	111	87	0	0.58	0.17	0.29	5	0	4	29	2.5

N/A = not acquired. Hb = Hemoglobin, FEV = Forced Expiratory Volume, TLco = Transfer Capacity of the lung for Carbon Monoxide, CT = Computed Tomography, RBC:TP = Red Blood Cell:Tissue/Plasma Ratio, STD = Standard Deviation, Coeff Var = Coefficient of Variation, mBORG = Modified BORG scale.

Table 2. Data for Each Post-Hospitalized Participant

ID	Age at scan (years)	Gender	Hb (g/L)	Time from infection (days)	FEV (%)	TLco(%)	CT Score	RBC:TP Mean	RBC:TP STD	RBC:TP Coeff Var	Dysp-12	mBORG pre	mBORG post	Number of resps in one minute	Percentile for Age and Sex
1	62	M	156	129	92	N/A	10	0.37	0.13	0.36	N/A	N/A	N/A	N/A	N/A
2	69	M	160	169	114	N/A	5	0.31	0.08	0.28	N/A	N/A	N/A	N/A	N/A
3	56	F	122	195	108	100	3	0.32	0.10	0.31	14	N/A	N/A	N/A	N/A
4	66	M	146	192	109	89	2	0.29	0.11	0.39	N/A	N/A	N/A	N/A	N/A
5	62	M	130	68	76	71	7	0.22	0.11	0.47	15	N/A	N/A	N/A	N/A
6	69	M	137	212	119	95	15	0.25	0.08	0.34	11	1	2	21	2.5
7	55	F	131	269	69	79	23	0.28	0.11	0.39	5	1	5	23	2.5
8	55	M	133	26	62	85	14	0.16	0.08	0.50	1	1	5	31	2.5
9	29	M	142	84	95	N/A	0	0.59	0.15	0.25	N/A	N/A	N/A	N/A	N/A
10	62	M	165	101	54	90	7	0.33	0.15	0.46	N/A	5	8	25	2.5
11	60	M	167	173	83	N/A	12	0.34	0.12	0.36	N/A	0	6	31	25
12	48	M	147	159	76	77	14	0.28	0.09	0.31	11	N/A	N/A	N/A	N/A

N/A = not acquired, Hb = Hemoglobin, FEV = Forced Expiratory Volume, Tlco = Transfer Capacity of the lung for Carbon Monoxide, CT = Computed Tomography, RBC:TP = Red Blood Cell:Tissue/Plasma Ratio, STD = Standard Deviation, Coeff Var = Coefficient of Variation, mBORG = Modified BORG scale.

Supplemental Materials

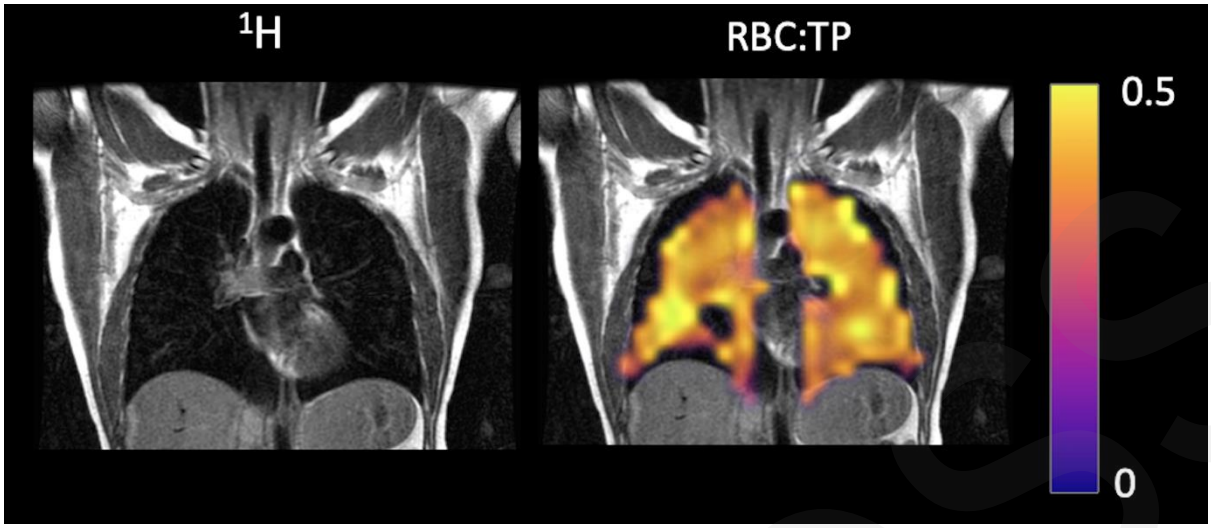

Figure E1. Example Proton (^{1}H) and fused RBC:TP map of a healthy participant in this study, showing highly homogeneous RBC:TP across the whole lungs.

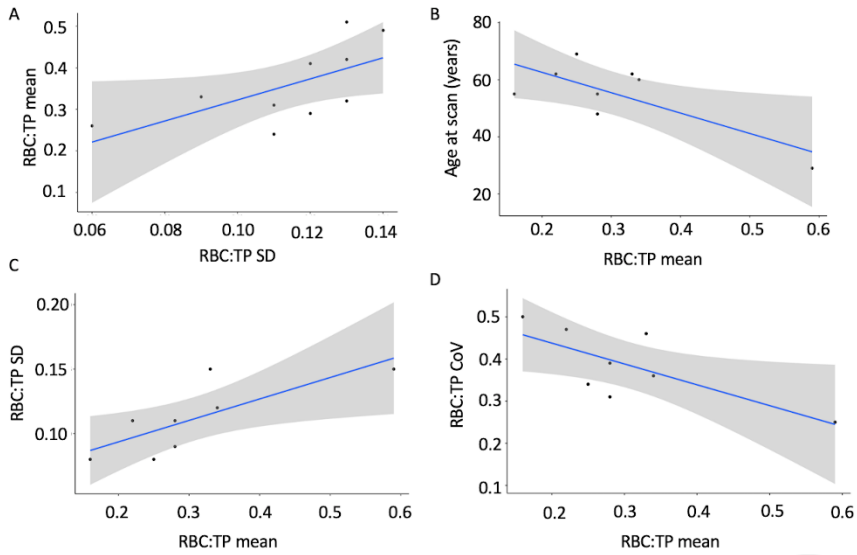

Figure E2. A significant positive correlation between RBC:TP mean and Standard Deviation (SD) in the NHLC group **(A)**. Significant correlations between Age and RBC:TP mean **(B)**, RBC:TP Sd and TBC:TP mean **(C)**, and RBC:TP Coefficient of Variation (CoV) and RBC:TP mean **(D)** in the PHC group. Results demonstrate that there is a decrease in RBC:TP with age, and that imaging metrics are internally consistent and reflect discernable changes in gas handling in the post-COVID lungs.

Table E1. Repeatability Data for Dissolved Phase Measurements

ID	RBC:TP mean at scan 1	RBC:TP mean at scan 2
1	0.37	0.37
2	0.31	0.29
3	0.32	0.29
4	0.29	0.33
5	0.22	0.24
6	0.25	0.26
7	0.28	0.28
8	0.24	0.23
9	0.44	0.45
10	0.14	0.17

RBC:TP = Red Blood Cell : Tissue/Plasma ratio.